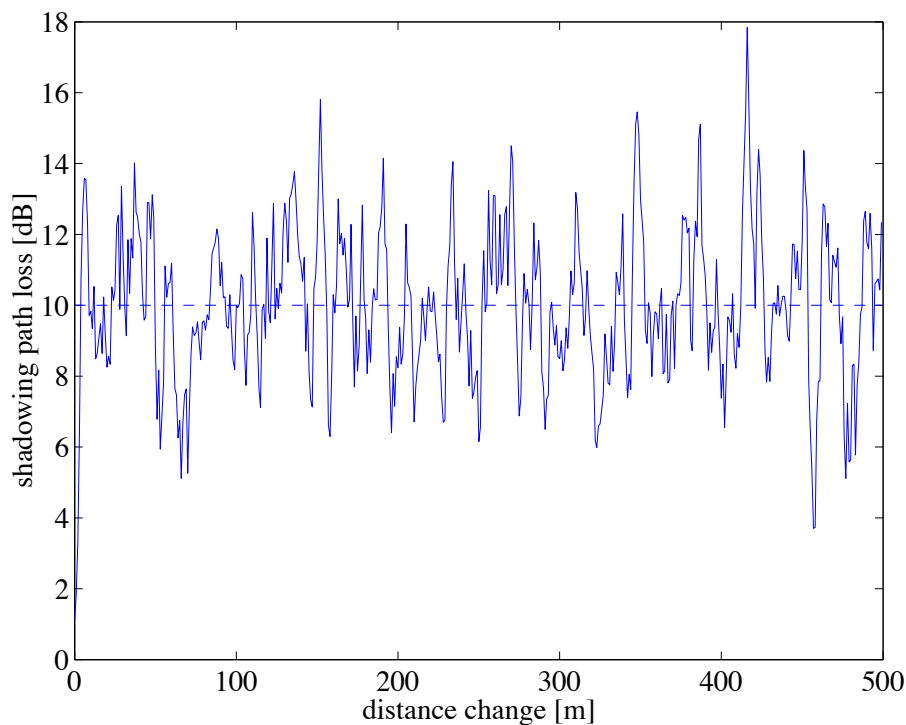


## 7.10 Fading Channels

### 7.10.1 Shadowing

Until now, we have covered the first of the multiplicative channel effects only, namely path loss. In our analysis so far we have assumed at most two paths, a direct one and a reflected one. In reality, however, there is usually a multitude of paths, making the problem hard to determine. Also, very often the exact surroundings may not be known. The approach sought is often statistical modeling. A complicated environment with several objects between transmitter and receiver make the outcome of a path-loss analysis highly dependent on the exact location of transmitter and receiver. Placing the receiver slightly to one side might produce a high difference in path loss, not predicted by our former models. This phenomenon is called *slow fading* or *shadowing*. A typical variation of path loss can be seen in Fig. 7.40. The probability distribution of the un-



**Figure 7.40** Typical shadowing path loss due to location variation of mobile receiver. Current example: median path loss = 10 dB (dashed line); path loss standard deviation (location variability)  $\sigma_L = 5$  dB.

derlying signal powers is log-normal, i.e., the loss expressed in dB has a normal distribution. The variation of the path loss occurs over distances comparable to object sizes, i.e., widths of buildings and hills and is called *location variability*  $\sigma_L$ . The reason for the log-normal distribution can easily be seen by considering the composition of the path loss by several independent effects on the way. Thus, the loss can be written as

$$L = L_1 \cdot L_2 \cdot L_3 \cdots L_N \quad (7.99)$$

in linear form, or in dB form as

$$L [\text{dB}] = L_1 [\text{dB}] + L_2 [\text{dB}] + L_3 [\text{dB}] + \dots + L_N [\text{dB}]. \quad (7.100)$$

If all of the  $N$  contributions are independent random variables, the central limit theorem dictates that  $L$  [dB] is a Gaussian random variable.

Shadowing has some impact on the link budget. If only the median path loss is used to evaluate a certain range covered, the real path loss exceeds the maximal value for reliable communications for 50 % of the cases. Hence, a certain *fade margin* has to be included in the link budget to make sure that most (you can never be 100 % sure but you can get very close to it) path losses incurred lead to successful communications. Thus, the fade margin to be included depends on the location variability and the percentage in desired successful communications.

### 7.10.2 Fast Fading

An even more dramatic effect than shadowing is *fast fading*, since it occurs on a much smaller time scale or with a much shorter correlation over location change. Since the relative bandwidth of a signal is usually very small, we analyze all fading effects in their complex baseband representation. The fading effects can then be conveniently modeled by complex phasors, indicating that fading changes amplitude and phase rapidly over time.

#### Flat Fading

With *flat fading*, we mean that there is only one path to consider (or at least several paths come in at such a short delay that they can be treated as one). The path loss parameter can therefore be accurately modeled by one time-varying complex scalar (amplitude and phase). Since such a multiplication influences the whole signal spectrum in the same way, flat fading is often also called *frequency nonselective fading*. As with shadowing, the path loss parameter has a statistical distribution. The kind of distribution depends on which one of two main cases we find: First, there is no line-of-sight path and the signal is the composition of a large number of random reflections, or, second, the random reflections are superimposed by a line-of-sight path.

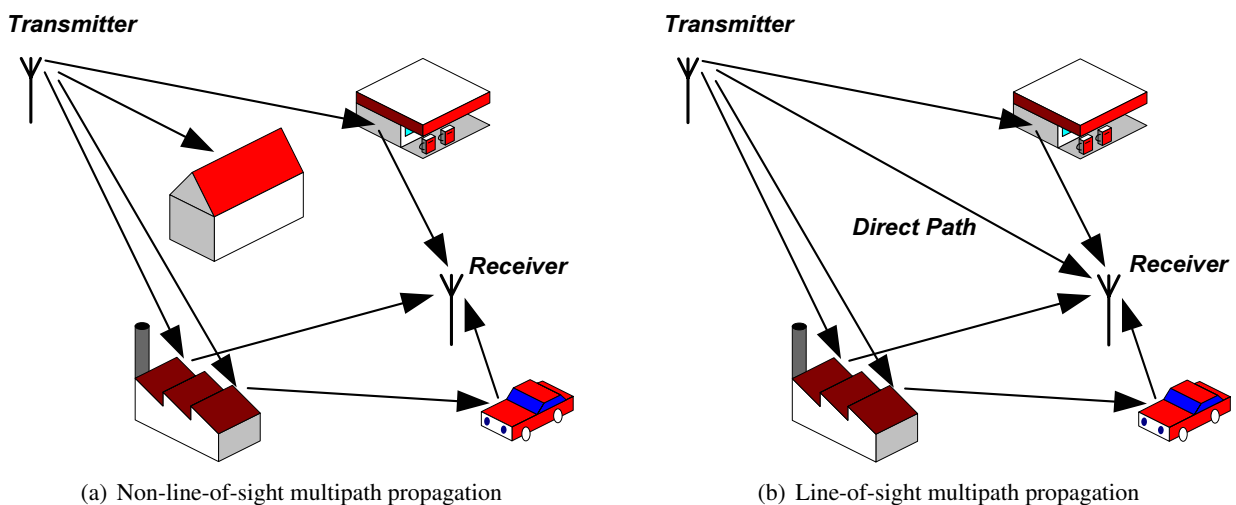


**Figure 7.41** The two types of multipath propagation.

Let us consider the first case, which is illustrated by Fig. 7.41(a). Note that as opposed to shadowing, where the composition of one path consisted of several multiplicative effects, we have now several paths adding up to a fluctuating, complex path-loss factor. Since the real part and the imaginary part of the complex path-loss factor (remember we model everything in the baseband) are independent processes, each of the part is a zero-mean Gaussian random variable. It can be shown that the corresponding distribution of the phase, essentially the argument of real and imaginary part, is uniformly distributed over  $[0 \dots 2\pi]$  and the amplitude  $r$  has a Rayleigh distribution given by its probability-density function (pdf)

$$p(r) = \frac{r}{\sigma^2} e^{-\frac{r^2}{2\sigma^2}}. \quad (7.101)$$

The pdf of the Rayleigh distribution is depicted by Fig. 7.42. Such a fading process is therefore termed Rayleigh fading. It concerns the loss factor  $L$  in the linear domain (not the dB domain).

In the second case, which is illustrated by Fig. 7.41(b), we have a strong line-of-sight signal in addition to the scatterer. The distribution of the amplitude is a Ricean distribution given as

$$p(r) = \frac{r}{\sigma^2} e^{-(r^2+s^2)/2\sigma^2} I_0\left(\frac{rs}{\sigma^2}\right), \quad (7.102)$$

where  $s^2 = m_1^2 + m_2^2$  is the noncentrality parameter consisting of the  $I$ - and  $Q$ -contribution of the signal present and  $I_0$  is the modified Bessel function of the first kind and degree zero. The pdf of the Rice distribution is also depicted by Fig. 7.42. As opposed to the Rayleigh distribution, the Rice distribution looks

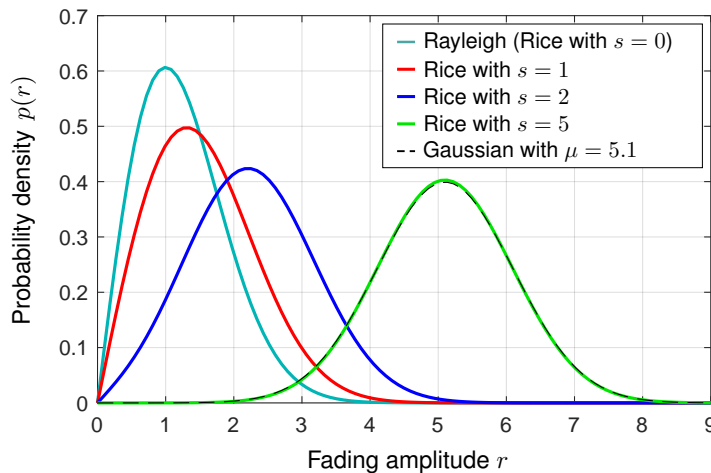


**Figure 7.42** Probability density functions of the Rayleigh and the Rice distributions. Both distributions are normalized to  $\sigma = 1$ .

much more symmetrical, due to the influence of the direct path. Still, no negative values are possible, so it is slightly asymmetrical. For large values of  $s$ , the Rice distribution can be accurately modeled by a Gaussian distribution.

The technique to evaluate the path loss due to fast fading is for either case the same as for shadowing: Specify the needed percentage (probability of successful communication) and evaluate the minimum amplitude via the cumulative density function (or the tail function). This amplitude then directly converts into a fast-fading power loss (or fade margin) to put into the link budget.

One direct application of the Rayleigh distribution given by Eq. (7.101) of a flat fading process is of direct interest to the communications engineer: the BER curve of a BPSK signal in a flat Rayleigh-fading channel.

We have seen in Chapter 3 that the BER of a BPSK signal is of the form

$$P_E(E_s/N_0) = P_E(\gamma) = Q\left(\sqrt{\frac{2E_s}{N_0}}\right). \quad (7.103)$$

and is clearly a function of the SNR as given by  $\gamma = \text{SNR} = E_s/N_0$ . The underlying assumption at the point of derivation was that the symbol energy was constant, leading to a constant  $\gamma$ . Now when there is fading, this is no longer true. It can be shown that if the amplitude is Rayleigh distributed, the SNR has a chi-square distribution with two degrees of freedom, which is an exponential distribution given by

$$p(\gamma) = \frac{1}{\Gamma} e^{-\frac{\gamma}{\Gamma}}, \quad (7.104)$$

where  $\Gamma$  is the average SNR of the fading process. We now have to evaluate a tail function, whose argument is exponentially distributed. The BER is then given as the expectation of the different BERs for varying SNR according to their distribution given by Eq. (7.104). Hence,

$$\begin{aligned} P_E &= E\{P_E(\gamma)\} \\ &= \int_0^\infty \frac{1}{\Gamma} e^{-\frac{\gamma}{\Gamma}} Q(\sqrt{2\gamma}) d\gamma \\ &= \int_0^\infty \frac{1}{\sqrt{2\pi}} \int_{\sqrt{2\gamma}}^\infty e^{-\frac{x^2}{2}} dx \frac{1}{\Gamma} e^{-\frac{\gamma}{\Gamma}} d\gamma \\ &= \frac{1}{\sqrt{2\pi}\Gamma} \int_0^\infty \int_0^{\frac{x^2}{2}} e^{-\frac{\gamma}{\Gamma}} d\gamma e^{-\frac{x^2}{2}} dx. \end{aligned} \quad (7.105)$$

The last equality is obtained by changing the integration order. The inner integral can now easily be computed. Hence,

$$\begin{aligned} P_E &= \frac{1}{\sqrt{2\pi}\Gamma} \int_0^\infty \Gamma \left(1 - e^{-\frac{x^2}{2\Gamma}}\right) e^{-\frac{x^2}{2}} dx \\ &= \frac{1}{\sqrt{2\pi}} \int_0^\infty e^{-\frac{x^2}{2}} - e^{-\frac{x^2}{2}\left(1+\frac{1}{\Gamma}\right)} dx \\ &= \frac{1}{2} - \frac{1}{2} \sqrt{\left(1 + \frac{1}{\Gamma}\right)^{-1}} \\ &= \frac{1}{2} \left(1 - \sqrt{\frac{\Gamma}{1+\Gamma}}\right). \end{aligned} \quad (7.106)$$

The result can be visualized in Fig. 7.43. The BER of a flat Rayleigh fading channel does not improve as fast as in the AWGN case when increasing the SNR. SERs/BERs of other binary modulation schemes are given in Table 7.4 without derivation.

The above modeling of a channel using Rayleigh and Rice distributions is in fact only half the truth. In addition to this, second-order statistics (essentially how fast the channel changes) have to be incorporated to make a channel model more realistic. The mechanism behind the fact that the fading process is correlated rather than white can be characterized by the *coherence time*, the time during which a channel is considered constant, which is inversely proportional to the *Doppler spread*, a channel characteristics that indicates how wide the frequency occupation of a signal is spread due to a moving transmitter, receiver, or both.

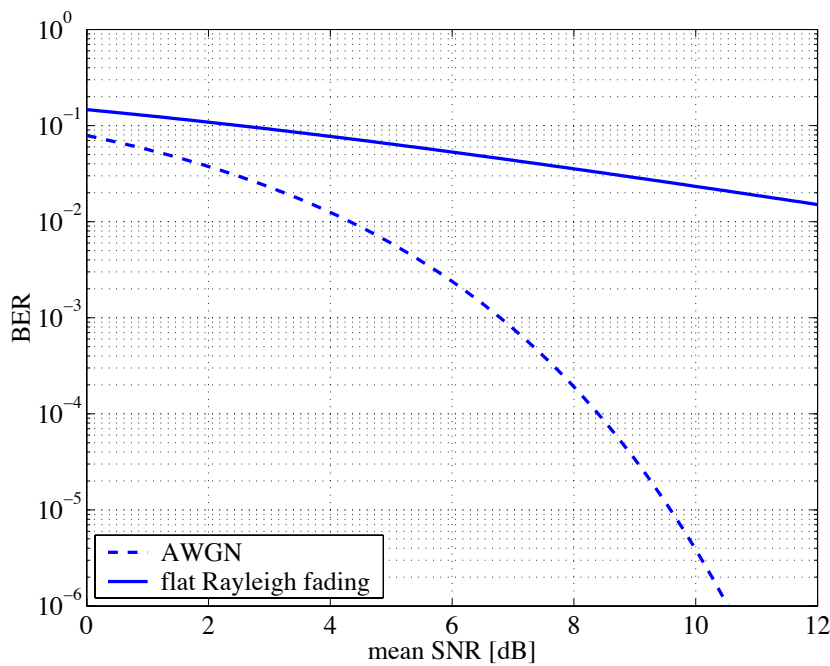


**Figure 7.43** Bit-error rates of a BPSK signal in the AWGN case and in a flat Rayleigh-fading channel, respectively.

Modulation	SER/BER (Rayleigh fading (flat))
BPSK	$\frac{1}{2} \left( 1 - \sqrt{\frac{\Gamma}{1+\Gamma}} \right)$
DPSK (noncoherent)	$\frac{1}{2(1+\Gamma)}$
2-FSK (orthogonal, coherent)	$\frac{1}{2} \left( 1 - \sqrt{\frac{\Gamma}{2+\Gamma}} \right)$
2-FSK (orthogonal, noncoherent)	$\frac{1}{2+\Gamma}$

**Table 7.4** SERs for some digital modulation formats in a flat Rayleigh-fading channel.

### Frequency-Selective Fading

As the delays between the individual paths of a multipath signal get larger with respect to the symbol duration, the fading process can no longer be considered flat, or frequency non-selective. In fact, with larger delays between rays, the channel becomes a wideband fast-fading channel or a *frequency-selective fading* channel. Such a channel can often be modeled by a baseband FIR filter, whose complex-valued taps are independently faded according to the statistics (either Rayleigh or Rice distributed as seen in the last section), see Fig. 7.44.

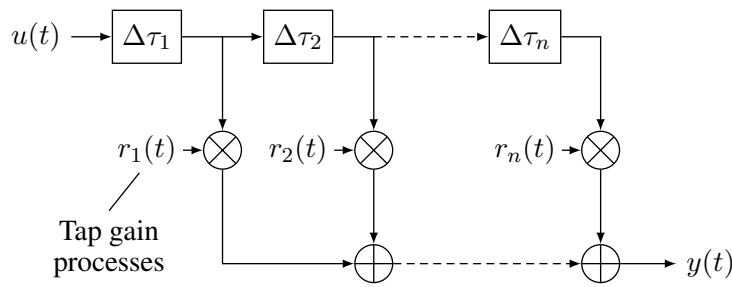


**Figure 7.44** Frequency-selective fading channel model.

The relationship between input and output is given by the convolution

$$y(t) = (h * u)(t) = \int h(\tau)u(t - \tau)d\tau, \tag{7.107}$$

where the impulse response of the wireless channel is

$$h(t) = \sum_{k=1}^n r_k(t)\delta(t - t_k). \tag{7.108}$$

The channel impulse response is often abbreviated as CIR in the literature. Its Fourier transform is called the channel transfer function (CTF). Note that the channel taps are both complex-valued and time-variant. The mean powers of the taps

$$P_k = E\{|r_k|^2\} \tag{7.109}$$

are usually given by a channel profile together with the corresponding delays, the so-called *power delay profile* (see Fig. 7.45), which is further characterized by the following parameters:

- *total excess delay*: the delay between the first and the last arriving tap response, essentially the amount by which the duration of a transmitted symbol is extended by the channel,

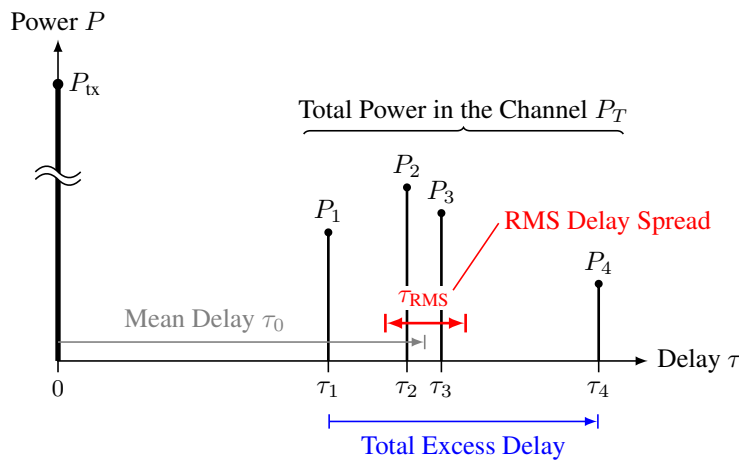


**Figure 7.45** Power delay profile.

- *mean delay* defined by

$$\tau_0 = \frac{1}{P_T} \sum_k P_k \tau_k, \quad (7.110)$$

where, compared to Fig. 7.44, we have

$$\tau_k = \sum_{l=1}^k \Delta \tau_l, \quad (7.111)$$

- *RMS delay spread* defined by

$$\tau_{\text{RMS}} = \sqrt{\frac{1}{P_T} \sum_k P_k (\tau_k - \tau_0)^2}, \quad (7.112)$$

where the total power in the channel is given by

$$P_T = \sum_k P_k. \quad (7.113)$$

The last parameter, the delay spread, is a good indicator of how frequency selective the channel is. It is inversely proportional to the *coherence bandwidth*. If the delay spread of a channel is much smaller than the symbol duration, the channel may be considered narrowband (flat fading). On the other hand, large delay spreads compared to symbol lengths mean that intersymbol interference (ISI) occurs, i.e., echos of a previous symbol overlap with the current incoming symbol.

### 7.10.3 Mobile Environment

In a truly mobile communication environment we face two challenges: Firstly, mountains, hills, and buildings lead to excessive delay spread, which in turn introduce frequency-selective fading. Secondly, changing the user position makes the channel response highly variable. An RF receiver usually needs to address both problems, the first one by providing a flexible structure that can essentially invert the channel, and the second one by providing an algorithm to track the channel changes. Such an equalizer structure is shown in Fig. 7.46.

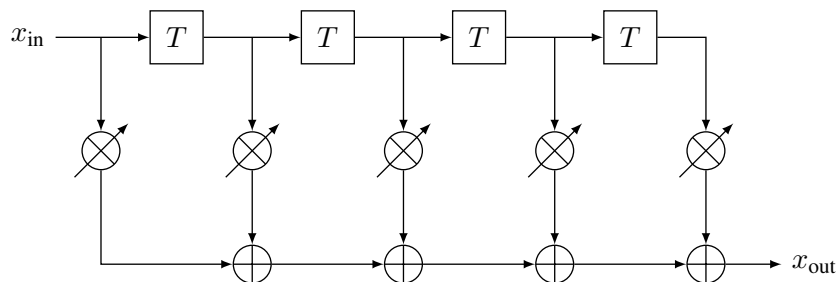


**Figure 7.46** Block diagram of a channel equalizer.

### 7.10.4 Relationship of Fading Parameters

In the last sections, we have encountered different types of fading. These types can be characterized by different parameters, some of which are related to each other.

The coherence time  $T_{\text{coh}}$ , which characterizes the time over which the channel transfer function stays essentially the same, and the Doppler spread, which describes the spectral broadening, are inversely related, thus

$$T_{\text{coh}} \propto \frac{1}{f_d}. \quad (7.114)$$

On the other hand, the coherence bandwidth  $B_{\text{coh}}$  determines the span over which the channel appears flat. Its inverse parameter, the delay spread  $\tau$  stands for the time broadening. Again these two parameters relate to each other as

$$B_{\text{coh}} \propto \frac{1}{\tau}. \quad (7.115)$$

In summary, for a given communication system with symbol time  $T$  and bandwidth  $B$  we can now build Table 7.5. Note that a fading channel can be at the same time one of the top two types and one of the bottom two types, hence, any one of four combinations is possible. In fact, the proportionality factors in

Fading type	Condition	Alternative formulation of condition
Flat fading	$B_{\text{coh}} \gg B$	$\tau \ll T$
Frequency-selective fading	$B_{\text{coh}} < B$	$\tau > T$
Slow fading	$T_{\text{coh}} \gg T$	$f_d \ll B$
Fast fading	$T_{\text{coh}} < T$	$f_d > B$

**Table 7.5** Fading types.

Eqs. (7.114) and (7.115) depend on the exact behavior of the channel impulse response and its variation in time, respectively. Rules of thumb are given by [56]

$$B_{\text{coh}} \approx \frac{1}{50\tau}, \quad (7.116)$$

if the frequency correlation function is above 0.9, and

$$B_{\text{coh}} \approx \frac{1}{5\tau}, \quad (7.117)$$

if the frequency correlation function is above 0.5. Sometimes, the relationship

$$B_{\text{coh}} \approx \frac{1}{2\pi\tau} \quad (7.118)$$

is also used. Very similar rules can be found for the relationship given by Eq. (7.114). Rappaport [56] states that

$$T_{\text{coh}} \approx \frac{9}{16\pi f_d} \quad (7.119)$$

for the time correlation to be above 0.5.



### 7.10.5 Examples of Channel Models

Channel models against which radio equipment are tested, are often given by standardization bodies. In the following, we list three typical channel models as standardized by ETSI for use in the GSM system. The 'x' stands for the speed, which does not, however, affect the tap model as such, but the underlying fading process.

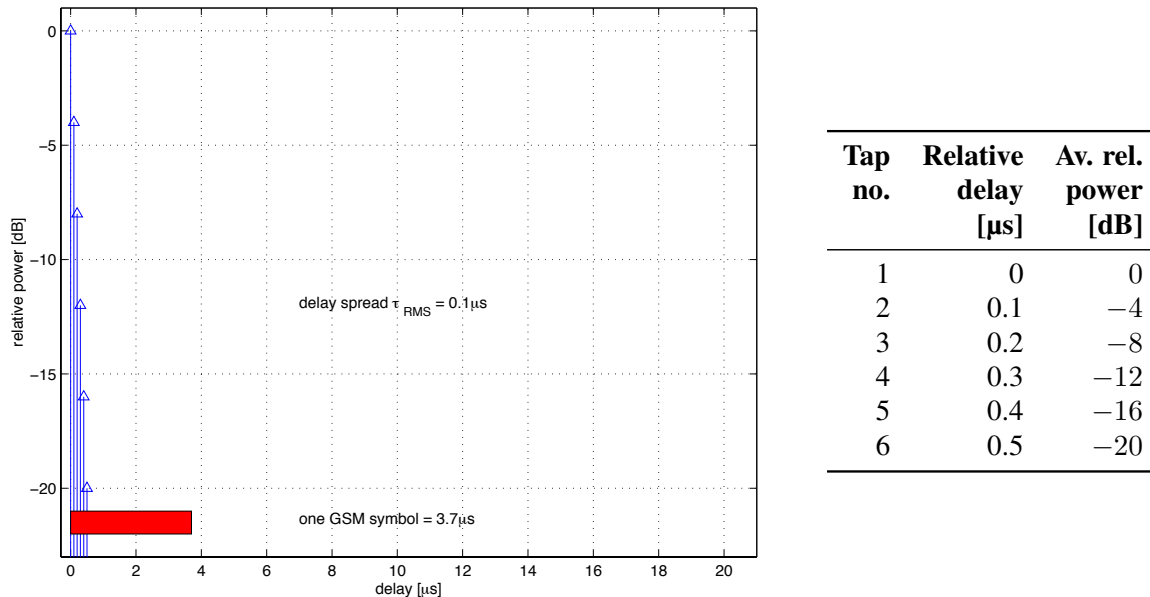


**Figure 7.47** Rural area (RAx) propagation model for GSM.

In Figs. 7.47 to 7.49 values for comparison with the symbol length used in GSM are given in both graphical and tabular form.

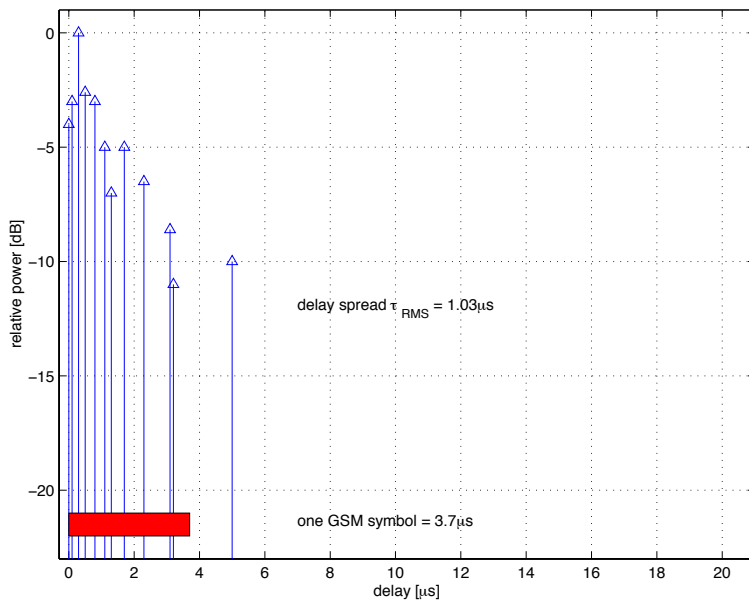
### 7.10.6 Ways Out

If we have to design a wireless communication system in such a hostile environment as mentioned above, we can either accept the situation and deploy a channel equalizer, or try to seek the situation where we do not need one. If we look at a typical snapshot of a channel frequency response, e.g., Fig. 7.50, we realize that the channel looks quite flat as long as we only use a narrow part (subband) of it, indicated by the region between the dashed lines. We then say that the bandwidth (of the subband) is smaller than the coherence bandwidth

$$W_{\text{sub}} \ll B_{\text{coh}}. \quad (7.120)$$

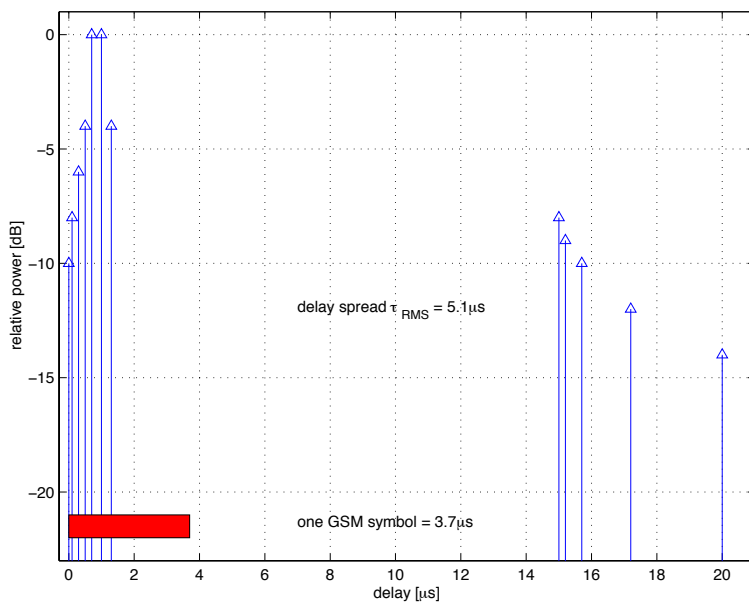
The idea of dividing the available bandwidth into a multitude of subbands that are smaller than the coherence bandwidth was realized by Chang [11] in the 60s. All we need to 'equalize' the channel in each 'flat' subband, is a variable factor, a complex-valued factor, in order to restore amplitude and phase. Why does this factor need to be variable? Well, because each subband may show a different attenuation to be compensated for.

Moreover, the attenuation may change, and so does the complex-valued factor we have to multiply the subband with. We better make sure the situation does not change within the duration of a symbol, otherwise



Tap no.	Relative delay [μs]	Av. rel. power [dB]
1	0	-4
2	0.1	-3
3	0.3	0
4	0.5	-2.6
5	0.8	-3
6	1.1	-5
7	1.3	-7
8	1.7	-5
9	2.3	-6.5
10	3.1	-8.6
11	3.2	-11
12	5	-10

Figure 7.48 Typical urban (TUx) propagation model for GSM.



Tap no.	Relative delay [μs]	Av. rel. power [dB]
1	0	-10
2	0.1	-8
3	0.3	-6
4	0.5	-4
5	0.7	0
6	1	0
7	1.3	-4
8	15	-8
9	15	-9
10	16	-10
11	17	-12
12	20	-14

Figure 7.49 Hilly terrain (HTx) propagation model for GSM.

we cannot determine the compensation factor. Hence, we have a second condition on the choice of our

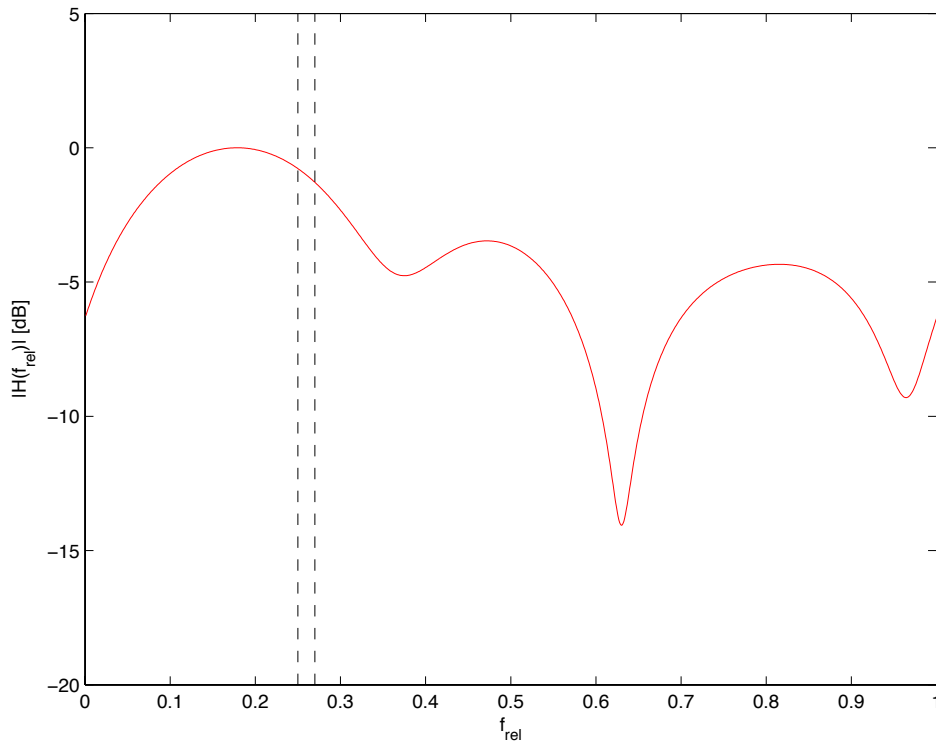


**Figure 7.50** Frequency response snapshot of a frequency-selective fading channel.

system. The duration of a symbol within a subband shall be much shorter than the coherence time

$$T_{\text{sub}} \ll T_{\text{coh}}. \quad (7.121)$$

Dividing a bandwidth  $W$  into  $N_c$  subbands delivers

$$W_{\text{sub}} = \frac{W}{N_c} \quad (7.122)$$

and

$$T_{\text{sub}} = \frac{1}{W_{\text{sub}}} = \frac{N_c}{W}. \quad (7.123)$$

Eqs. (7.120) and (7.121) now deliver

$$\frac{W}{N_c} \ll B_{\text{coh}}, \quad (7.124)$$

$$\frac{N_c}{W} \ll T_{\text{coh}}. \quad (7.125)$$

Combined into one inequality we finally get

$$\frac{W}{B_{\text{coh}}} \ll N_c \ll WT_{\text{coh}}. \quad (7.126)$$

We thus get lower and upper limits for the choice of the number of subchannels  $N_c$ . This consideration was already used when OFDM was introduced in Section 3.2.